



Original Article

Target strength of skipjack tuna (*Katsuwonus pelamis*) associated with fish aggregating devices (FADs)

Guillermo Boyra^{1*}, Gala Moreno², Bea Sobradillo¹, Isabel Pérez-Arjona³, Igor Sancristobal¹, and David A. Demer⁴

¹Azti Foundation, Herrera kaia, Portualdea z/g, Pasaia 20110, Spain

²International Seafood Sustainability Foundation (ISSF), 601 New Jersey Ave NW Suite 220, Washington, DC 20001, USA

³Dept. de Física Aplicada, IGIC Universitat Politècnica de València, Valencia, Spain

⁴Southwest Fisheries Science Center, National Oceanic and Atmospheric Administration, 8901 La Jolla Shores Drive, La Jolla, CA 92037, USA

*Corresponding author: tel: + 34 667 174 436; fax: (+34) 94 657 25 55; e-mail: gboyra@azti.es

Boyra, G., Moreno, G., Sobradillo, B., Pérez-Arjona, I., Sancristobal, I., and Demer, D. A. Target strength of skipjack tuna (*Katsuwonus pelamis*) associated with fish aggregating devices (FADs). – ICES Journal of Marine Science, 75: 1790–1802.

Received 20 April 2017; revised 24 February 2018; accepted 13 March 2018; advance access publication 17 April 2018.

This paper presents measures of target strength (TS; dB re 1 m²) and models of TS vs. fork length (L ; cm), i.e. $TS = 20\log(L) + b_{20}$, for skipjack tuna associated with fish aggregating devices (FADs) in the Central Pacific Ocean. Measurements were made using 38-, 120-, and 200-kHz split-beam echosounders on a purse-seine workboat during fishing operations. To mitigate potential bias due to unresolved targets, TS measurements were rejected if they were not simultaneously detected with multiple echosounder frequencies in approximately the same location. The filtered TS and concomitantly sampled L data were used to estimate $b_{20} = -76, -71,$ and -70.5 dB for 38, 120, and 200 kHz, respectively, using the method of least squares. For comparison, quasi-independent estimates of TS and b_{20} were calculated from acoustic echo-integration and catch data representing entire aggregations around the FADs. The results differed by ≤ 1 dB for all three frequencies. The sensitivities of these results to variations in fish morphology and behaviour were explored using a simulation of TS for fish without swimbladders. The utility of the results on acoustic properties of skipjack tuna and next research steps to achieve selective fishing at FADs are discussed.

Keywords: acoustics, echosounder, FAD, frequency response, multiple targets, selectivity, sonar, split beam, tropical tuna, tuna

Introduction

Fish aggregating devices (FADs) are used to catch tropical tunas, skipjack (*Katsuwonus pelamis*) comprising more than half of the global tuna catch. Almost invariably, skipjack are found with bigeye (*Thunnus obesus*) and yellowfin tuna (*Thunnus albacares*) at FADs (Fonteneau *et al.*, 2013). Although the stocks of skipjack are reported to be in healthy condition, recent stock assessments for bigeye and yellowfin tuna indicate that these tuna stocks are fully exploited or subject to overfishing in different regions (ISSF, 2017).

In recent years, the widespread use of FADs to catch skipjack has motivated increased efforts to minimize catches of bigeye, yellowfin, and other non-target species (bycatch). One approach is to use the fishers' echosounders, sonars, and echosounder buoys

(Lopez *et al.*, 2014; Moreno *et al.*, 2016) to not only locate and fish on target species, but also to identify the presence and distribution of non-target species near FADs before nets are set. Data from these instruments could also be used to estimate tuna distributions and abundances to inform stock assessments (Moreno *et al.*, 2016). To quantitatively interpret acoustic data collected around FADs, it is necessary to know the sound scattering characteristics of the target species. In particular, echo-integration estimates of fish abundance requires knowledge of mean target strength [$TS = 10\log(\sigma_{bs});$ dB re 1 m²], where σ_{bs} (m²) is the backscattering cross-section (MacLennan *et al.*, 2002), vs. acoustic frequency (f ; kHz) and fish length (L ; cm) (Simmonds and MacLennan, 2005). Models of $TS(f)$ can be used to allocate

echoes to target species (Korneliussen, 2010), potentially facilitating more selective fishing, and models of $TS(L)$ can be used to convert nautical area backscatter coefficients (s_A ; m^2/nmi^2) to estimated animal densities (Simmonds and MacLennan, 2005).

Despite the importance of characterizing TS vs. f and L , measures of tuna around FADs have generally been made with only a single frequency (e.g. Doray *et al.*, 2006; Josse and Bertrand, 2000; Moreno *et al.*, 2008), and there have been no published $TS(f)$ and $TS(L)$ models for *in situ* skipjack. This lack of knowledge prevents both fishers and scientists from interpreting data provided by the acoustic tools used when fishing or studying fish at FADs. To improve this situation, a series of scientific cruises promoted by the International Seafood Sustainability Foundation were conducted onboard commercial purse seiners to study sound scattering properties of tropical tuna species around FADs. In this study we focus on skipjack tuna, the main target species associated with FADs. Using data from almost pure sets of skipjack collected in a Central Pacific Ocean cruise in 2014, we provide modelled $TS(f)$ and $TS(L)$ relationships for skipjack using two different approaches, as well as interpretation of the obtained results based on fish-backscattering simulations.

Methods

Data collection

Acoustic data

Sonar (Furuno FSV84), and purse-seine catch data were collected in the Central Pacific Ocean, aboard F/V *Albatun 3*, between 3 and 31 May 2014. During this period, data were also collected from 38-, 120-, and 200-kHz echosounders (Simrad EK60) mounted on the vessel's 8-m workboat, with the transducers (Simrad ES38-12, ES120-7C, and ES200-7C, respectively) projecting vertically downward (Figure 1). The echosounders were calibrated using a 38.1-mm diameter sphere made from tungsten carbide with 6% cobalt binder (Demer *et al.*, 2015; Foote, 1987), and configured with the calibrated parameters (Table 1) prior to data collections.

Ten minutes before and throughout each of 20 purse-seine sets, the workboat was attached to the drifting FAD, and TS and volume backscattering strength (S_V ; dB re 1 m^{-1}) data were collected from 5- to 200-m depth. During the ~60-min sets, the workboat slowly towed the FAD to maintain separations from the net and the vessel.

Purse-seine catch data

Skipjack schools were captured using an 1800-m long \times 310-m deep purse-seine net. During the second half of each set, two divers visually observed the species in the shallowest 25 m of the aggregation. While the catch was lifted aboard, 1–2 tons of fish was sampled, generally from every sixth or seventh brail, into a fiberglass box (110 \times 70 \times 100 cm). Fish species were identified and fork lengths, L , were measured (1-cm precision) using flat measuring boards. For each species, fish weights (w ; g) were estimated from the measured L and a model of $L(w)$ (Cayré and Laloë, 1986). The catch weight for each species was estimated by multiplying the weight proportion for each species and the fishing master's estimate of total-catch tonnage for the set.

Data analysis

Echosounder, sonar, and catch data from three purse-seine sets with $\geq 96\%$ skipjack by number ($\geq 94\%$ by weight) (Table 2) were processed using commercial (Echoview; Hobart, Tasmania)

and open source software (R, R Core Team, 2014). The TS and S_V data were analysed from ~5 min before the set until echoes from the net were visible at the bottom of the echogram (i.e. before the tuna changed their behaviour in response to the closing net).

Target selection

A routine was then applied to assure that the subsequent TS measurements were of pure skipjack targets. To avoid echoes from bycatch fish species, S_V and TS data were excluded if shallower than 25 m (Muir *et al.*, 2012; Forget *et al.*, 2015), deeper than 200m, or below echoes from the net. In addition, a school detection algorithm (Lawson *et al.*, 2001) was then used to retain the main aggregation (assumed to be skipjack, given the high proportion of the catch). The rejected echoes from outside the aggregation were considered non-fish echoes (putative plankton or small nekton) that tend not to aggregate, or large bigeye and yellowfin, which tend to locate below the main aggregation (as described by Moreno *et al.*, 2008; Govinden *et al.*, 2010; Muir *et al.*, 2012; Lopez *et al.*, 2016) (Figure 2). After smoothing by an unweighted, normalized to unity, 5×5 convolution, "schools" (i.e. the main aggregations around the FAD) were selected using: minimum total school length and height = 0.2 m; minimum candidate length and height = 0.1 m; and maximum vertical and horizontal linking distances = 5 and 20 m, respectively. The school detection was applied on both S_V and TS echograms, and data from within the schools were attributed to skipjack (Figure 2).

TS estimation based on single targets

The TS echograms at each frequency were processed using a single-target detection algorithm (SIMRAD, 1996; Soule *et al.*, 1997) configured with the following settings: minimum threshold = -80 dB; normalized pulse durations = 0.9–1.5; maximum off-axis angles = 3° ; and maximum standard deviations of phase = 0.6° .

Multiple-target rejection

To mitigate bias in TS measurements due to unresolved targets (Demer *et al.*, 1999), the single-target detections were filtered further using the following methods:

- (1) Standard deviation (SD): Alongships and athwartships phase was thresholded (Soule *et al.*, 1997) with values ranging from 0.9° – 0.1° .
- (2) Fish tracking (FT): TS measurement sequences were ascribed to individual fish using a method (Blackman, 1986) applied in commercial software (Echoview; Myriax Inc., Hobart, Tasmania) and configured with the following parameters (Moreno *et al.*, 2008): ≥ 3 consecutive detections; ≤ 5 missing pings; missed ping expansion = 0%; sensitivity to unpredicted change in position, $\alpha = 0.7$; sensitivity to velocity, $\beta = 0.5$; exclusion distances along major and minor axes = 4 m; target-to-track assignment weights = 30 (major axis), 30 (minor axis), and 40 (vertical axis); and ≤ 1 m inter-ping depth variation. The latter corresponds to the maximum vertical velocities recorded for tuna during ultrasonic tracking experiments around moored FADs (Cayré and Chabanne, 1986; Marsac and Cayré, 1998).

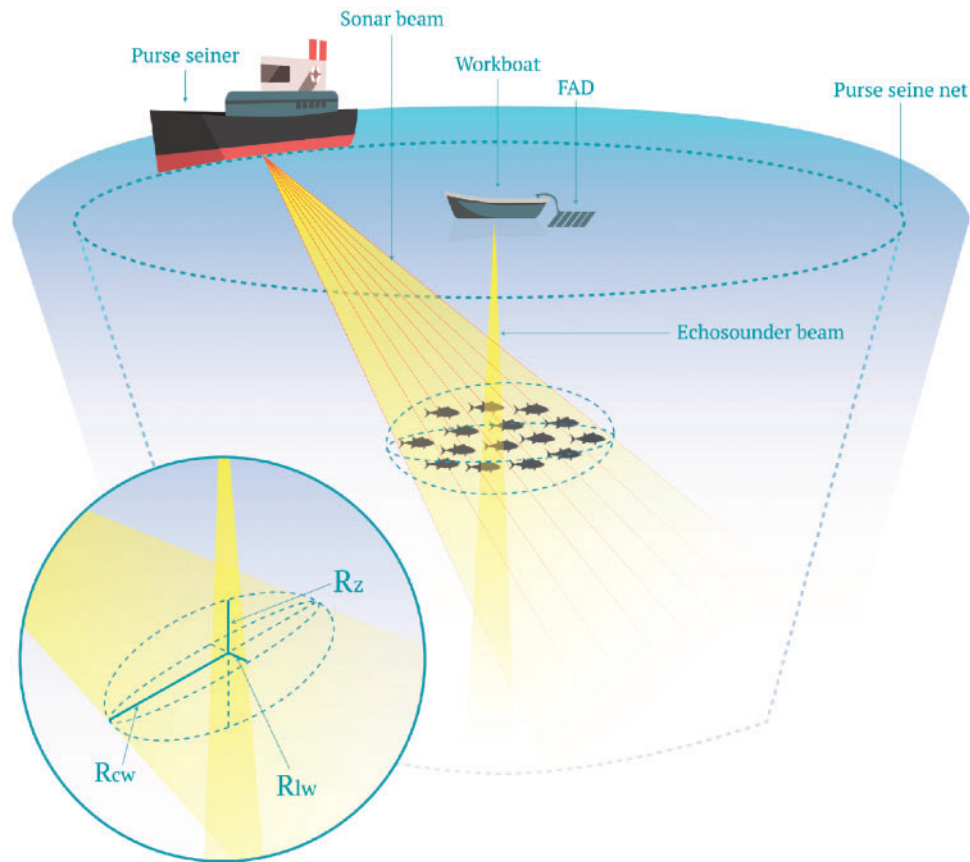


Figure 1. For each of 20 purse-seine sets, echosounders on a workboat were used to measure target strength (TS; dB re 1 m^2), volume backscattering strength (S_V ; dB re 1 m^{-1}), and school height ($2R_z$; m) for skipjack beneath the FAD; and a scanning sonar on a purse-seine vessel was used to estimate the school width ($2R_{cw}$; m) and length ($2R_{lw}$; m).

Table 1. Calibrated echosounder (Simrad EK60) settings used to measure target strength (TS; dB re 1 m^2), volume backscattering strength (S_V ; dB re 1 m^{-1}).

Frequency (kHz)	38	120	200
Pulse duration (μs)	512	512	512
Power (W)	2000	250	150
Gain (dB)	26.16	25.96	27.09
Sa correction (dB)	-0.86	-0.39	-0.34
Ath. beam angle (deg)	6.92	6.38	6.43
Along beam angle (deg)	6.94	6.39	6.37
Sphere TS (dB)	42.3	40	39.9
TS deviation (dB)	5	5	5
RMS beam model	0.19	0.18	0.20
RMS polynomial model	0.16	0.16	0.15

(3) Multiple frequencies simultaneously (MFS): TS measurements were accepted if concomitantly detected by multiple frequencies (Demer *et al.*, 1999). First, the relative transducer positions were determined (Conti *et al.*, 2005) using sphere echoes recorded simultaneously at multiple frequencies, and a non-linear optimization (Powell, 1994) implemented in the R (R Core Team, 2014) package “NLOptr” (Johnson, n.d.). Then, the target coordinates were transformed into a common coordinate system (Conti *et al.*, 2005). The minimum distance

between detections by different frequencies was varied sequentially from 5 to 0.01 m.

(4) High fish density (HFD): TS measurements were accepted if they were from areas with low fish densities (Sawada *et al.*, 1993). The threshold fish density was determined by plotting the number of single targets per cell (T_V) against the total number of fish per cell (N_V) and choosing (Gauthier and Rose, 2001) the N_V that produced a peak in T_V . This procedure assures that the threshold density is independent of the TS value used to calculate it. The threshold was evaluated for grid-cell dimensions ranging from 1500 ($10 \text{ m} \times 100$ pings; 1 ping $\approx 0.15 \text{ m}$) to 3.0 m^2 ($10 \text{ m} \times 2$ pings).

TS(L) and TS(f) relationships

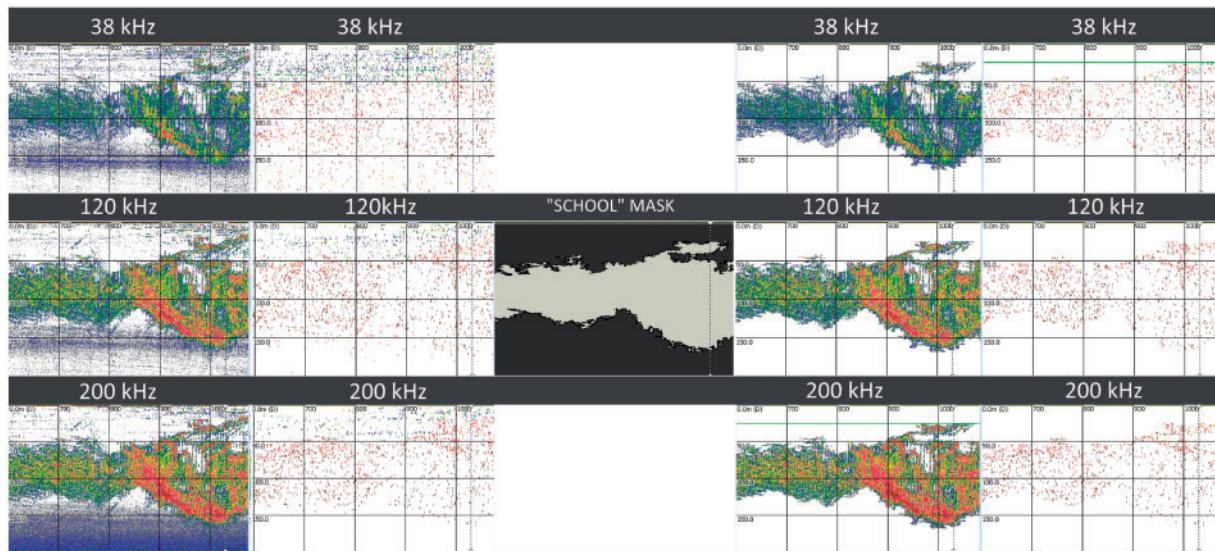
After filtering echoes from multiple targets, TS(L) was modelled as

$$\text{TS} = 20\log(L) + b_{20}, \quad (1)$$

where b_{20} (Simmonds and MacLennan, 2005) of skipjack was estimated for each frequency using the *in situ* TS distributions, measurements of L distribution from the purse-seine catches (Fernandes *et al.*, 2006), and the method of least squares (MacLennan and Menz, 1996). The slope in (1) was assumed to be 20 (Simmonds and MacLennan, 2005) because the inter-set differences in mean L ($< 3 \text{ cm}$) were too small to estimate its

Table 2. Proportions and mean lengths of skipjack (SKJ), bigeye (BET), and yellowfin tuna (YFT) in three catches that included $\geq 96\%$ SKJ by number ($\geq 94\%$ by weight).

Set ID	Catch (tons)	Weight proportion (%)			Number proportion (%)			Mean Fork Length (cm)		
		SKJ	BET	YFT	SKJ	BET	YFT	SKJ	BET	YFT
24	170	100	0	0	99	1	0	48	32	49
26	125	94	4	2	97	2	1	52	58	62
27	170	94	4	2	96	2	2	49	55	47

**Figure 2.** The procedure to attribute echoes to skipjack, illustrated by data from set ID 24. The original S_V and TS echograms (columns 1 and 2) were filtered using a school detection algorithm, converted to a mask (column 3, row 2) applied to the S_V (column 4) and TS (column 5) echograms, resulting in data for putative skipjack tuna. Minimum display thresholds = 70 dB.

value from the data. Standard deviations, calculated with the R package “Seewave” (Sueur et al., 2013), confidence intervals of the TS distributions, and coefficient of determination values of the TS(L) models were calculated.

TS estimation based on volume backscatter

Mean TS was independently estimated for each of the three frequencies and purse-seine catches by inverting the volume backscatter equation (Misund and Beltestad, 1996),

$$TS \text{ [dB re } 1 \text{ m}^2] = 10\log(S_V wV/B), \quad (2)$$

where S_V is the volume backscattering coefficient (m^2/m^3), w is the mean weight of skipjack in the spill sample (g), B is the skipjack biomass in the catch (g), and V is the ellipsoidal volume of the skipjack aggregation (m^3),

$$V = (4/3)\pi R_{cw}R_{lw}R_z, \quad (3)$$

where the average school height (R_z ; m) is estimated from the S_V echogram (Figure 1), and the school width (R_{cw} ; m) and length (R_{lw} ; m), assumed to be equal, are estimated from horizontal range in a sonar image (e.g. Figure 3) recorded at the beginning of the set, scaled and corrected for distortion according to the

procedure of Misund (1993). The school width was made equal to the length one instead of calculating it from the screen because the crosswise dimensions of the schools obtained from the sonar screenshots were slightly but consistently higher than the lengthwise ones, thus indicating a likely poorer effectiveness of the distortion correction (and thus slightly biased estimation) in this direction.

TS sensitivity

TS of a bladderless fish is not only a function of acoustic frequency and fish size, but also shape, material properties (flesh, bone, and other organs) and behaviour (Gorska et al., 2005; Korneliussen, 2010). To have a better understanding of the factors that contribute to the TS of bladderless species in general and skipjack tuna in particular, finite element models (FEM) (Jech et al., 2015) were run to predict *in situ* TS measurements of skipjack tuna. However, due to the paucity of published material properties for this species, the simulations were run in comparison with Atlantic mackerel, a more studied bladderless fish (Gorska et al., 2005) that was taken as a reference. The simulations were run by pairs, one for Atlantic mackerel, considered as a baseline, and a second one obtained by changing only one of the model parameters of Atlantic mackerel to suitable values for skipjack. The resulting change in b_{20} in each pair informed on

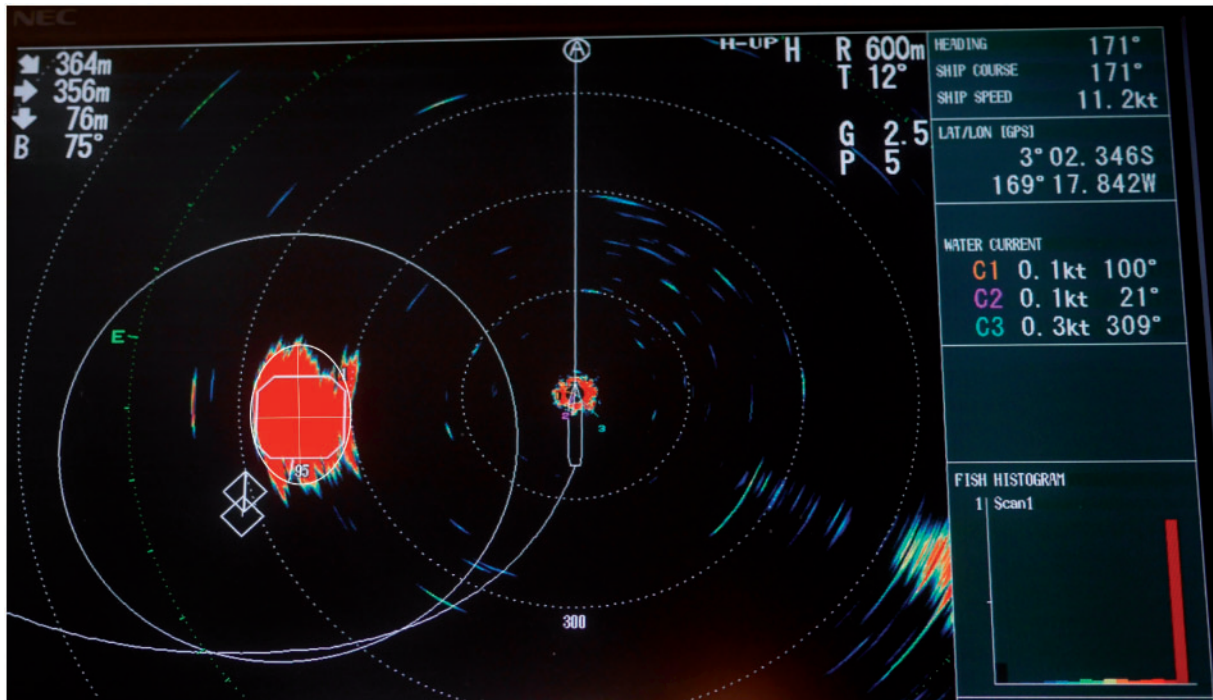


Figure 3. Example sonar image (set ID 24) showing the position of the purse-seine vessel (centre of the concentric dashed-line circles) and the horizontal ranges to and across a skipjack school (large red patch) beneath the FAD.

which individual properties could theoretically contribute more to the TS differences between the two species. The goal of the simulations, rather than obtaining the best match with the experimental results, was to understand which parameters can contribute more to the TS of fish species when the swimbladder is absent.

For Atlantic mackerel, published density and sound speed values of flesh and backbone were used (Gorska *et al.*, 2007; Sigfusson *et al.*, 2001a) (Table 3). For skipjack, we used albacore tuna (*Thunnus alalunga*) values (Table 3) for flesh sound speed (Sigfusson *et al.*, 2001b) and density (Alexander, 2013). Arbitrary values were used for the backbone, assumed more rigid and dense than for Atlantic mackerel, to match the qualitative impression obtained cutting slices of specimens of both species. The FEM models were solved using $L = 20$ cm, and $f = 18, 38, 70$, and 80 kHz for both species.

Shape was modelled as an ellipsoid (flesh only, model code A, Table 3), an ellipsoid with an internal cylinder (flesh and bone, model code B), and outlines of X-ray images of one specimen of each species (model code C). For computational efficiency, only longitudinal waves were considered along the backbone (Forland *et al.*, 2014a, b). Convergence was assessed with ≥ 20 nodes per wavelength. Evaluations at higher frequencies required more computer memory than was available (Jech *et al.*, 2015).

Model sensitivities were evaluated for: equivalent shape and different flesh properties (model code A.1, Table 3); equivalent shape and bone but different flesh properties (B.1); equivalent shape and flesh but different backbone properties (B.2); equivalent shape but different flesh and bone properties (B.3); equivalent shape, flesh and bone properties, but different incidence angle distributions (B.4); equivalent flesh and bone properties and incidence angle distributions, but different shapes from

X-ray images (C.1) (Figure 4); and equivalent flesh and bone properties, but different shapes (from X-ray images) and incidence angle distributions (C.2) (Table 3).

Results

TS measurements

The procedure to isolate skipjack tuna echoes transformed the multimodal TS measurements, which include TS of putative plankton, small nekton and bycatch species, to unimodal distributions (Figure 5).

The efficiency of each of the four methods applied to remove unresolved targets was as follows:

- (1) Decreasing the standard deviation of split-beam phase (SD) decreased the number of 38 kHz detections but did not change the mean TS (Figure 6). Therefore, either the mean TS is not biased from multiple targets or decreasing the standard deviation of split-beam phase $< 0.9^\circ$ did not eliminate multiple targets. Therefore, this threshold was set equal to the default value of 0.6° .
- (2) Increasing the number of fish detections per track (FT) to 8 decreased the mean TS; and larger numbers of fish detections per track increased both the mean TS and the standard error (s.e.) (Figure 6). Because it was not possible to visually confirm that the tracks were from individual fish and not artefacts of the large number of detections within the aggregation, FT was not considered further.
- (3) For simultaneous detections at multiple frequencies (MFS), decreasing the allowable distance between targets to ~ 0.15 m decreased the mean TS; and shorter distances increased both

Table 3. Model parameters and average b_{20} values.

Models		Body (flesh) parameters					Bone parameters				b_{20} @ f (kHz)							
Code	Type	Body shape	Tested element	FAO code	Inc. angle (°)	Length (cm)	Height (cm)	Width (cm)	ρ (kg/l)	c (m/s)	Length (cm)	Diameter (cm)	ρ (kg/l)	c (m/s)	18 (dB)	38 (dB)	70 (dB)	80 (dB)
A.1	F	Ellipsoid	Flesh	MAC	90±5	20	3.6	3	1.06	1537	—	—	—	—	-80.52	-82.22	-85.02	-79.32
A.1	F	Ellipsoid	Flesh	"SKJ"	90±5	20	3.6	3	1.09	1600	—	—	—	—	-74.02	-76.32	-74.42	-74.02
B.1	F&B	Ellipsoid	Flesh	MAC	90±5	20	3.6	3	1.06	1537	18	0.36	1.13	2600	-77.12	-87.92	-70.82	-71.72
B.1	F&B	Ellipsoid	Flesh	"SKJ"	90±5	20	3.6	3	1.09	1600	18	0.36	1.13	2600	-72.22	-78.12	-68.22	-73.02
B.2	F&B	Ellipsoid	Bone	MAC	90±5	20	3.6	3	1.06	1537	18	0.36	1.13	2600	-72.22	-78.12	-68.22	-73.02
B.2	F&B	Ellipsoid	Bone	"SKJ"	90±5	20	3.6	3	1.06	1537	18	0.36	1.3	3200	-71.92	-76.72	-66.62	-71.12
B.3	F&B	Ellipsoid	Flesh and bone	MAC	90±5	20	3.6	3	1.06	1537	18	0.36	1.13	2600	-77.12	-82.82	-70.82	-71.72
B.3	F&B	Ellipsoid	Flesh and bone	"SKJ"	90±5	20	3.6	3	1.09	1600	18	0.36	1.3	3200	-71.92	-76.72	-66.62	-71.12
B.4	F&B	Ellipsoid	Incidence angle	MAC	90±5	20	3.6	3	1.06	1537	18	0.36	1.13	2600	-77.12	-87.92	-70.82	-71.72
B.4	F&B	Ellipsoid	Incidence angle	"SKJ"	90±10	20	3.6	3	1.06	1537	18	0.36	1.13	2600	-77.72	-85.62	-73.12	-72.72
C.1	F&B	X-ray	Shape	MAC	90±5	20	4.2	2.8	1.06	1537	14.9	0.35	1.13	2600	-79.32	-83.32	-77.62	-73.62
C.1	F&B	X-ray	Shape	"SKJ"	90±5	20	5	4.8	1.06	1537	17.17	0.38	1.13	2600	-78.52	-86.52	-76.12	-73.42
C.2	F&B	X-ray	Incidence angle	MAC	90±5	20	4.2	2.8	1.06	1537	14.9	0.35	1.13	2600	-79.42	-83.32	-77.52	-73.62
C.2	F&B	X-ray	Incidence angle	"SKJ"	90±10	20	5	4.8	1.06	1537	17.17	0.38	1.13	2600	-78.92	-85.72	-76.22	-74.12

For all models, the values assumed for seawater density and sound speed were $\rho = 1.030$ kg/l and $c = 1490$ m/s. For each Code (defined in the text), the Type is either F (only flesh) or F&B (flesh and bone). The FAO code is either MAC (Atlantic mackerel) or "SKJ" (skipjack tuna; the quotations marks are a note to the reader that the parameters are not necessarily appropriate for skipjack tuna).

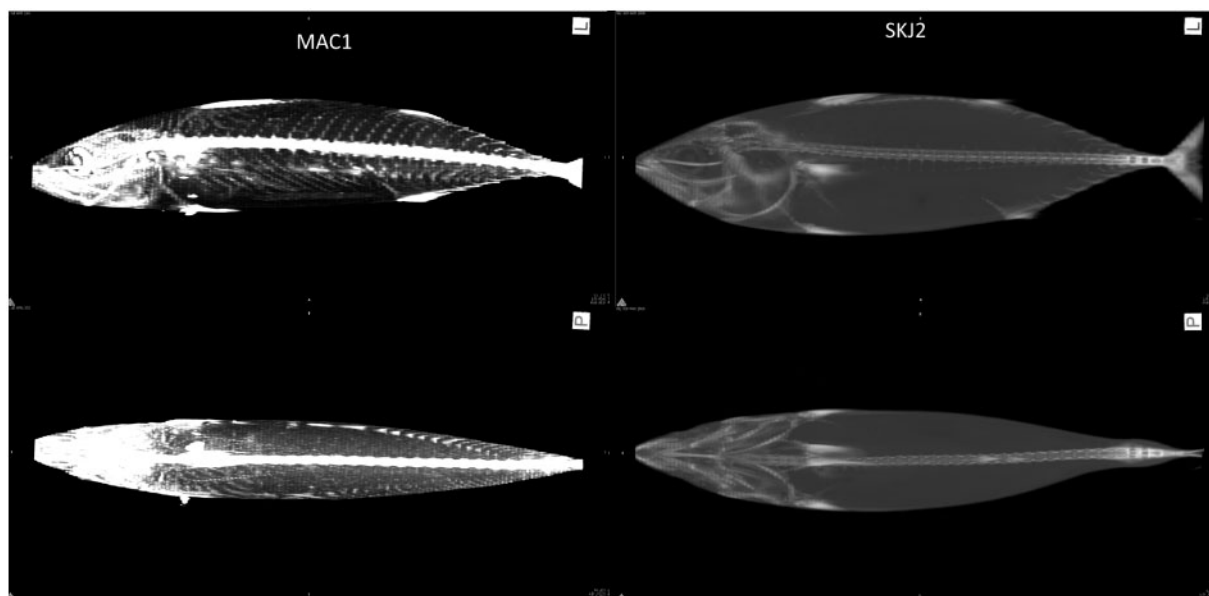


Figure 4. Dorsal (top row) and lateral (bottom row) X-ray images of Atlantic mackerel (left column) and skipjack tuna (right column) specimens with length, height, and width dimensions: 26.94, 5.26, and 3.86 cm (MAC1); and 41.8, 10.26, and 7.23 cm (SKJ2). (Note: X-rays for both species were taken using different settings, and are thus not directly comparable).

the mean TS and the SE (Figure 6). This indicated an optimal distance threshold for filtering multiple targets.

- (4) Decreasing the grid size for determining the high-density threshold (HDF) decreased the mean TS until the

minimum usable grid size was reached (10 m × 2 pings) (Figure 6). Because mean TS did not stabilize prior to reaching this smallest usable grid size, HDF was not considered further.

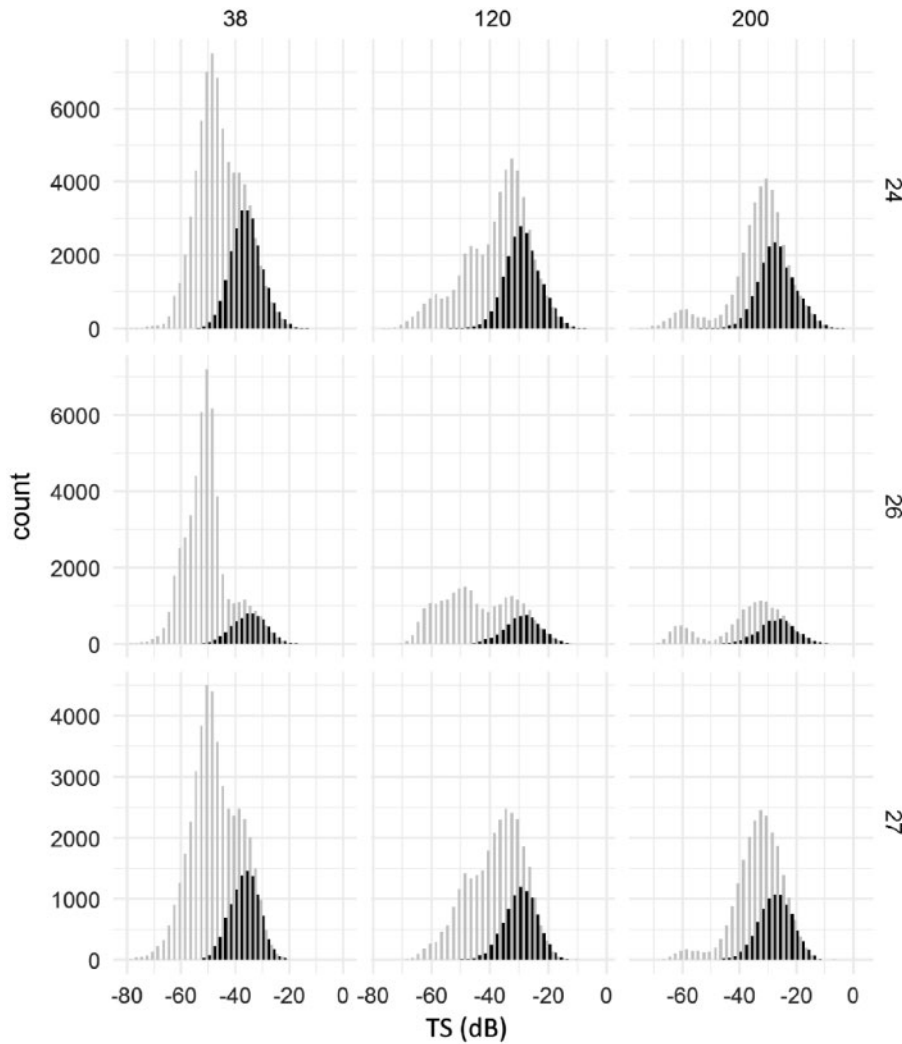


Figure 5. TS distributions for each frequency (columns) and set (rows), before (grey) and after (black) the school filter was applied to identify echoes from skipjack tuna. The lower intensity modes are likely from plankton and small nekton. On an average, about 2/3 of the data were removed in this step.

Among the methods tested to filter multiple targets, only MFS reduced bias in mean TS using an objectively defined threshold. Therefore, the results of the MFS filtering were used to fit $TS(L)$ models for each frequency. The mean TS values did not change along the set duration (results not shown).

$TS(L)$ and $TS(f)$ models

The $TS(L)$ relationships based on data passing the single target discrimination filters, have b_{20} values equal to -76 , -71 , and -70.5 dB for the 38, 120, and 200 kHz, respectively. Adjustment between observed TS distributions and those derived from (1) with measurements of L (Figure 7) with the least squares method have coefficients of determination (R^2) $\sim 80\%$ (Table 4 and Figure 8). Values of b_{20} derived by echo-integration using (2) and (3) were ~ 1 dB higher at all frequencies (Table 4). From measurements of single targets, TS of *in situ* skipjack tuna at 38 kHz is ~ 5 and ~ 5.5 dB lower than at 120 and 200 kHz, respectively (Figure 9); whereas from echo-integration, the TS at 38 kHz is ~ 5 and ~ 6 dB lower than at 120 and 200 kHz, respectively (Table 4). The uncertainties were lower for TS measurements of single

targets ($SD = 7, 6,$ and 6 dB at 38, 120, and 200 kHz, respectively) than for TS measurements derived from echo-integrations ($SD = 15, 8,$ and 7 dB, respectively).

TS sensitivities

In the FEM models, in general, TS decreased from 18 to 38 kHz, then increased with higher frequencies, the frequency response showing generally larger values at high (70–80 kHz) compared to low (18–38 kHz) frequencies for both species (Table 3). This increase at higher frequencies was not accentuated by the inclusion of a backbone.

Considering the comparison between skipjack and Atlantic mackerel at 38 kHz (the only simulated frequency that was directly comparable with the experimental results), larger values for flesh density and sound speed increased TS by 5–10 dB (Table 3). These models (A.1, B.2, and B.3) predicted b_{20} values within ~ 1 dB of the observed ones (Tables 3 and 4). Larger values for bone density and sound speed also increased TS, but by less than 2 dB. In contrast, TS did not increase with differences in shape nor a wider distribution of incidence angles (Table 3).

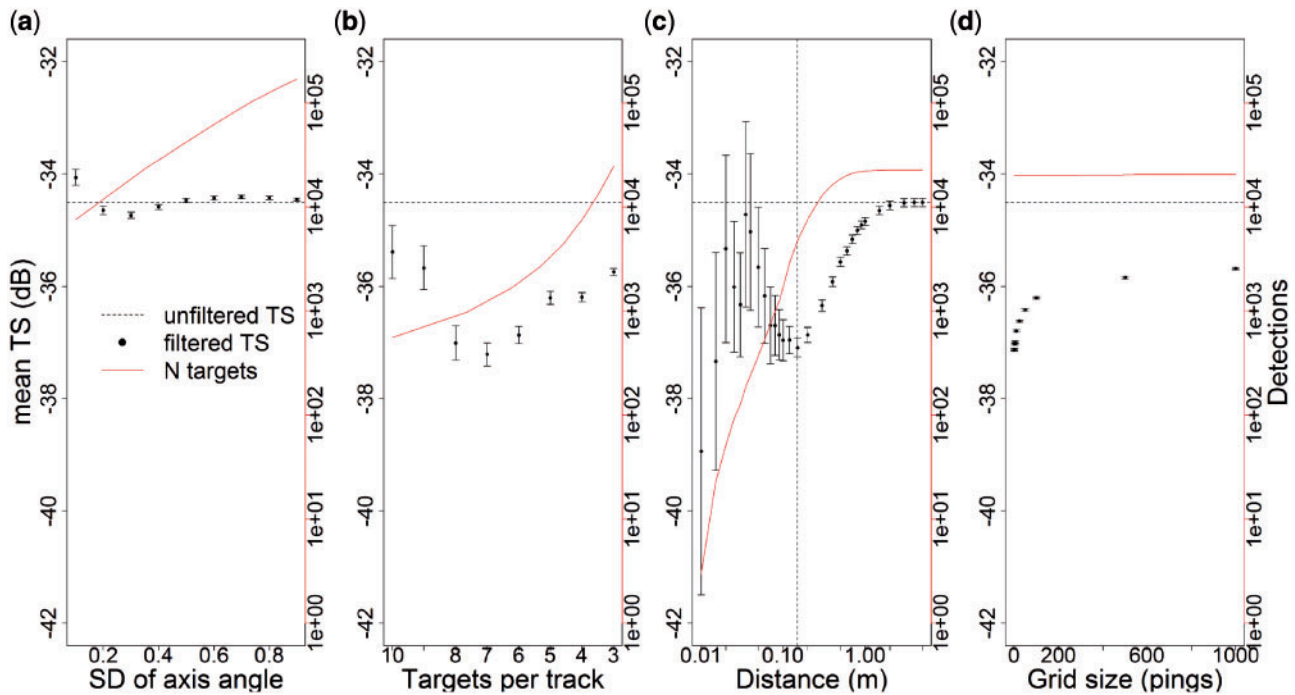


Figure 6. Mean TS for *in situ* skipjack measured at 38 kHz vs. standard deviation of split-beam phase (SD), number of targets per track (FT), distance between simultaneous detections at multiple frequencies (MFS), and grid size used to determine a HDF. Horizontal dotted line represents the unfiltered mean TS value. The number of TS measurements included in the average (continuous red line and right axis label) decreases, and the standard error increases (bars) with increased filter constraints. For MFS, the TS stabilized with a distance threshold of 0.15 m (vertical black line) at 38 kHz and 0.09 and 0.1 m at 120 and 200 kHz respectively (not shown).

Discussion

Experimental measurements

TS measurements of *in situ* fish may be biased due to inclusion of non-target species or multiple targets (Soule *et al.*, 1997; Demer *et al.*, 1999). Here, we use vertical stratification and a school detection algorithm to filter echoes from plankton, micro-necton and by-catch species and, after evaluating several methods, apply a multiple-frequency TS-detection method to filter multiple targets (Demer *et al.*, 1999; Conti *et al.*, 2005). The school detection algorithm filtered non-target echoes from above the skipjack school, likely from small tunas and other species (Forget *et al.*, 2015; Muir *et al.*, 2012; diver observations), and below the school, potentially larger bigeye and yellowfin tuna (Moreno *et al.*, 2008; Govinden *et al.*, 2010; Muir *et al.*, 2012). The sensitivity analyses for each of the filtering steps served to evaluate their effectiveness and optimize their parameters. For the MFS filter, we refined earlier works (Demer *et al.*, 1999; Conti *et al.*, 2005) by optimizing a threshold on the distance between simultaneous detections of candidate single targets. The school and MFS filters reduced the TS-measurement biases by ~ 2 –4 dB and, although they also reduced the number of targets by two orders of magnitude, the adjustment between predicted and observed TS values with the method of least squares provided high ($\sim 80\%$) coefficients of determination (Figure 8).

The echo-integration estimates of skipjack tuna TS were based on various important assumptions: (1) that the skipper's biomass estimates were accurate and precise, (2) that the schools had equivalent horizontal dimensions (i.e. $R_{cw} = R_{lw}$) and (3) that the measurement of a single sonar screenshot gives a reliable measurement of the horizontal aggregation size. The accuracy of the tonnage estimates for each set is unknown because multiple

catches are stored in the same hold, but their combined tonnage typically differs by $\sim 5\%$ from the total discharge weight (pers. comm., fishing company representative). Perhaps the measurement accuracy obtained with this approach could be improved by weighting entire catches ashore. It could also be improved by correcting bias in the measurements made perpendicular to the sonar beams, thereby allowing estimates of both horizontal dimensions of the school. And, finally, by averaging the measurements of horizontal school dimensions throughout the sets instead of using measures taken at the beginning of each set.

Despite the aforementioned uncertainties, the quasi-independent single-target-detection and echo-integration methods for estimating TS produced b_{20} values for skipjack tuna that were within ~ 1 dB (33%) of each other at all frequencies (Table 4). However, because of the assumptions of the echo-integration approach and their higher uncertainty (Table 4), the results from the single-target approach should be used to identify echoes from skipjack tuna and estimate their number densities.

This work compares the results of TS(L) models estimated using the single target discrimination and echo-integration methods, which are quasi-independent and have different sources of uncertainty. Therefore, similar results corroborate each other. Besides, the capability of the TS values to obtain accurate biomass estimations is implicitly tested in the echo-integration method. Therefore, the results of this study should facilitate unbiased acoustic estimates skipjack biomass.

Theoretical interpretation of skipjack TS

Our 38-kHz TS measurements of *in situ* skipjack tuna are ~ 2.5 dB lower than the mean TS measured for one skipjack tuna

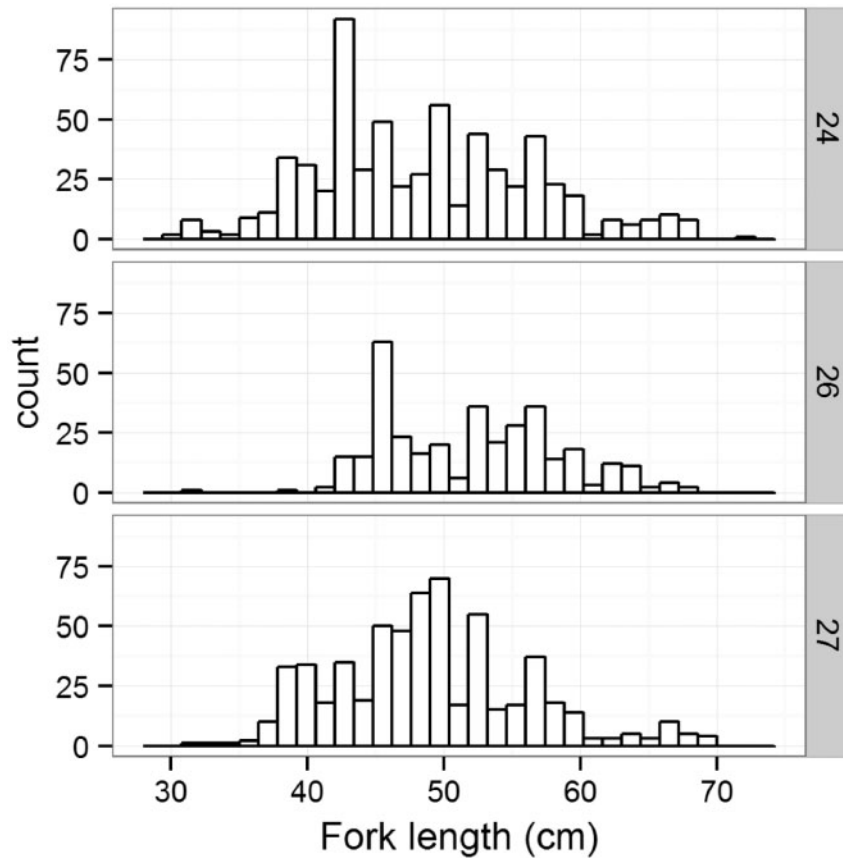


Figure 7. Distributions of fork length for skipjack tuna ranged from 30 to 70 cm in three catches (sets number 24, 26, and 27) that included $\geq 96\%$ skipjack tuna by number ($\geq 94\%$ by weight) (see Table 3).

in a cage (Oshima, 2008). The FEM model sensitivity analysis showed that this difference could be due to differences in material properties or incidence angle distributions for skipjack tuna aggregated near FADs vs. those for one captive specimen.

Our 38-kHz estimate of mean b_{20} for *in situ* skipjack tuna (-76 dB) is higher than values reported for Atlantic mackerel (*Scomber scombrus*), i.e. -90 dB (Scouling *et al.*, 2016), -88 dB (Clay and Castonguay, 1996), -86 dB (Fernandes *et al.*, 2006), -84.9 or -82 dB (ICES, 2006). The FEM model results (Table 3) predict b_{20} for skipjack higher than that of Atlantic mackerel. According to the simulations, the material properties can account for difference in b_{20} of up to ~ 10 dB at 38 kHz (model B.1). From those, acoustic properties of flesh accounted for the main b_{20} difference between both species, followed by backbone properties. In contrast, variations in shape and incidence angle distribution may have relatively little effect on the difference in TS of skipjack tuna vs. Atlantic mackerel (Table 3). It is possible, however, that a 5° change in the standard deviation of the incidence angle distribution in the model does not reflect the true range of natural behaviour for skipjack.

Some of the tested models matched the experimental results rather well (within <1 dB), whereas other models yielded very different results (up to 10 dB). However, as mentioned earlier, the goal of the simulations was not to match the experimental results in absolute terms, but rather to help interpreting them in terms of the relative contribution of different parameters to the TS of bladderless fish. In this regard, the 10 dB difference predicted for

different flesh properties (density and sound speed) alone can justify the differences between our results and TS of Atlantic mackerel found in bibliography.

However, these simulation results should be taken with caution due to the mentioned scarcity of information on material properties of skipjack. Overall, skipjack is known to be denser than Atlantic mackerel based on their respective length–weight relationships (Cayré & Laloë, 1986; Coull *et al.*, 1989) but it is not clear how much of this density difference is attributable to the bone and the flesh. Consequently, the values chosen for flesh properties (i.e. the parameters with the highest contribution to the TS) were taken from another tuna species, albacore tuna, of similar size. The rigidity of the backbone appears to be considerably higher for skipjack, but it has not been measured. Consequently, future studies should include direct measurements of skipjack flesh and bone properties for a range of fish lengths (e.g. Forland *et al.*, 2014b) and measurements of their orientation distributions.

Although the magnitude of skipjack TS differs from that of Atlantic mackerel, its $TS(f)$ resembles that of many species without swimbladders (Mosteiro *et al.*, 2004; Fernandes *et al.*, 2006; Korneliussen, 2010; Forland *et al.*, 2014a). However, because skipjack tuna are larger than Atlantic mackerel, the 5 and 5.5 dB increases in skipjack tuna TS at 120 and 200 kHz relative to 38 kHz (Figure 9) may be larger than for Atlantic mackerel (Gorska *et al.*, 2005, 2007). This $TS(f)$ for skipjack tuna is also different from that of fish species with swimbladders (Fernandes

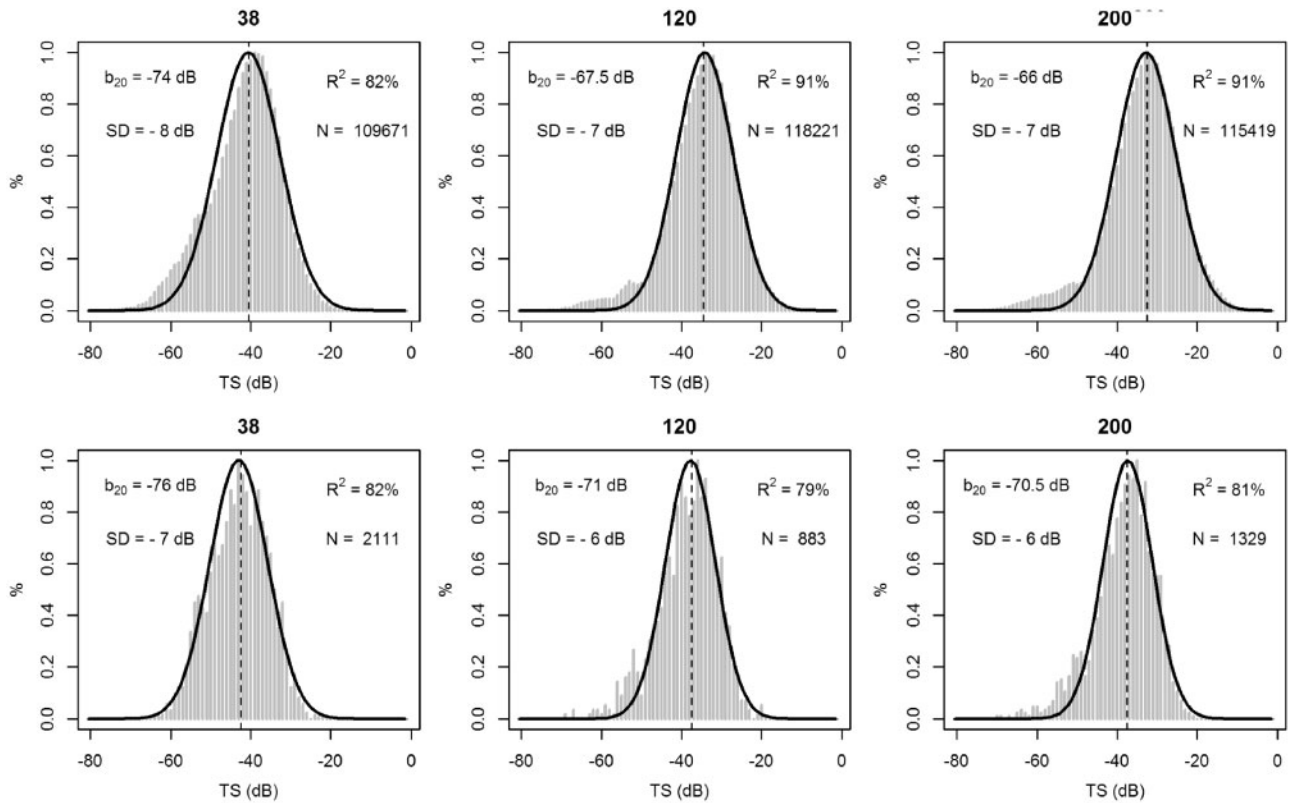


Figure 8. TS distributions of *in situ* skipjack tuna measured at 38, 120, and 200 kHz. To mitigate bias due to measurements of multiple targets, the split-beam detections (top row) were filtered to retain those (N = number remaining) that were simultaneously detected at multiple frequencies (bottom row). As in MacLennan and Menz (1996), each dataset was fit with a normal distribution (black lines) to evaluate the mean (dashed vertical line), standard deviation (SD) and b_{20} of the best fit, given by coefficient of determination (R^2), of observed vs. modelled TS distributions.

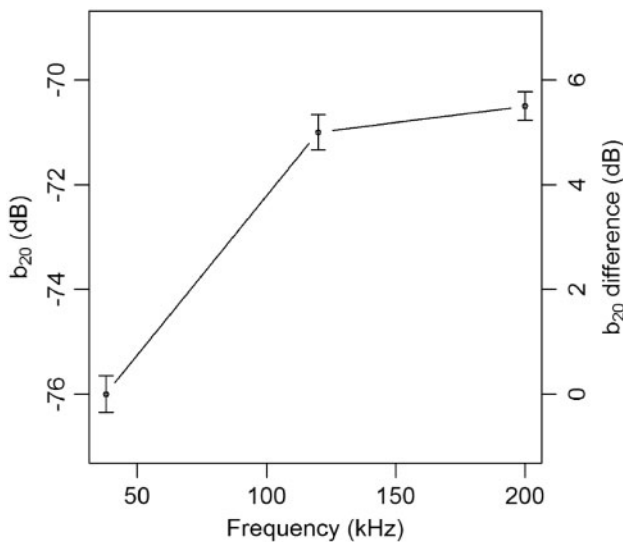


Figure 9. Measured b_{20} for skipjack tuna associated with FADs. The error bars (CI for b_{20} measurements) at 38 kHz don't overlap with those at 120 or 200 kHz, indicating significantly different (Cumming *et al.*, 2007) response between low and high frequencies. This pattern could be potentially useful for discriminating this species acoustically.

et al., 2006; Horne *et al.*, 2009). As skipjack is the main tuna species without swimbladder associated with FADs, this could be used to acoustically discriminate it from the other tuna species.

Use of acoustic data to support the sustainable fishing of tropical tunas

Bigeye and yellowfin tuna, the most abundant tuna species found at FADs, together with skipjack, are subject to overfishing in different regions. Informing fishers about the relative abundance of skipjack compared with that of yellowfin and bigeye could allow fishers to avoid setting nets on large abundances of species of concern.

The $TS(f)$ and $TS(L)$ relationships obtained for skipjack in this study are useful to improve the interpretation of the acoustic data collected by purse seiners fishing at FADs. However, the knowledge acquired is not enough: to provide acoustic estimations of abundance per tuna species, $TS(f)$ and $TS(L)$ of the other main tuna species found at FADs are also needed. $TS(L)$ relationships at 38 kHz are available for bigeye and yellowfin tuna from previous works (Bertrand *et al.*, 1999; Josse and Bertrand, 2000), but their $TS(f)$ are absent from bibliography and should be studied.

Given that our measurements were made *in situ* under real commercial fishery conditions, the obtained $TS(L)$ relationships reflect the true values of skipjack and be directly usable to

Table 4. Mean TS, standard deviation (SD), and best fit b_{20} values for *in situ* skipjack tuna at three acoustic frequencies (f), estimated from measurements of echo-integration and single targets.

Set ID	f (kHz)	Catch		Echo-integration					Single targets					
		L (cm)	B (t)	S_V ($10^{-6} \times 1/m$)	$R_{cw} = R_{lw}$ (m)	R_z (m)	TS (dB)	b_{20} (dB)	SD (dB)	TS (dB)	b_{20} (dB)	SD (dB)	CI (dB)	R^2 (%)
24	38	48	170	3.7	68	65	-43	-77						
26	38	52	118	3.2	66	44	-43	-77						
27	38	49	160	3.3	67	64	-43	-77						
All	38	50					-43	-77	15	-41	-76	8	(-76.5, -75.5)	82
24	120	48	170	11.1	68	65	-38	-72						
26	120	52	118	11.8	66	44	-37	-72						
27	120	49	160	9.3	67	64	-39	-73						
All	120	50					-38	-72	8	-37	-71	5	(-71.5, -70.5)	79
24	200	48	170	14.8	68	65	-37	-71						
26	200	52	118	13.5	66	44	-37	-71						
27	200	49	160	14.4	67	64	-37	-71						
All	200	50					-37	-71	7	-36.5	-70.5	5	(-71, -70)	81

For single targets, values are also shown for confidence interval (CI) and coefficient of determination (R^2) for the observed vs. expected TS distributions (Figure 8). The parameters for the echo-integration method include volume backscattering coefficient (S_V), school width (R_{cw}), length (R_{lw}), and height (R_z), estimated catch biomass (B), and mean fork length (L).

estimate skipjack abundance. The acoustic abundance estimation is obtained by isolating the biomass in (2), which leaves σ_{bs} (i.e. the linearized TS) at the denominator. The standard error of the measured σ_{bs} is $\sim 5\%$ at the three frequencies. As the variance of a quotient equals the sum of the variances of numerator and denominator plus their covariance in relative terms (Seber, 1982), assuming independence between the variances of the factors in (2), the uncertainty of the measured σ_{bs} alone would cause confidence intervals for the biomass $\sim 10\%$ around the mean (Cumming *et al.*, 2007).

To estimate the abundances of multiple species typically aggregated beneath FADs, it is necessary to first estimate the proportions of each species present. To do this, the frequency response of the aggregation may be compared with a mixed TS(f) model derived from a proportion (x) of the skipjack TS(f) model and proportion ($1 - x$) of a swimbladder fish TS(f) model, where the difference is minimized by optimizing x (e.g. Korneliusson, 2010). To increase the precision of the species proportion estimations, the mixed TS(f) model could include proportions of models for the other tuna species (e.g. Korneliusson *et al.*, 2016). The estimated proportions can then be used, analogous to species proportions in catches, to estimate abundances for each of the species following standard procedure (Simmonds and MacLennan, 2005).

Conclusion

The application of fish school and MFS filters on single-target detections at 38, 120, and 200 kHz served to mitigate measurement bias of TS distributions of skipjack tuna associated with FADs. The combination of echosounder, sonar, and net-sample measurements allowed inversion of the echo-integration equation to provide quasi-independent TS estimates. Values of b_{20} derived from these two methods differed by < 1 dB at all three frequencies. The TS(f) measured in this study is useful to estimate abundance of this species at FADs and to distinguish the echoes from skipjack tuna from tuna species with swimbladders, e.g. bigeye and yellowfin tunas, before purse-seine fishing at FADs. This

manuscript represents the first of a series of studies on the acoustic properties of tropical tunas, with the final goal of providing estimates of tuna abundance at FADs by species, suitable for selective fishing and fisheries independent estimates of tropical tuna abundance.

Acknowledgements

We thank the following organizations and people for their support of this work: the governments of Kiribati, Tuvalu, and Tokelau which permitted this research in their EEZs; Albacora for allowing this work aboard F/V ALBATUN TRES; Fishing Master Euken Mujika; the captain and crew; the scientists and divers J. Filmlalter and F. Forget are thanked for invaluable insight about fish behaviour, vertical stratification and non-target species composition at FADs; Hector Peña for providing instruction on the sonar setup and analysis; Yolanda Lacalle for the illustration in Figure 2; and Andres Uriarte for advice concerning transmission of statistical errors. The research reported in the present document was funded by the International Seafood Sustainability Foundation (ISSF) and conducted independently by the authors. The report and its results, professional opinions and conclusions are solely the work of the authors. This paper is contribution 843 from AZTI (Marine or Food Research).

References

- Alexander, R. 2013. Locomotion of Animals. Springer Science & Business Media.
- Bertrand, A., Josse, E., Massé, J., and Masse, J. 1999. In situ acoustic target-strength measurement of bigeye (*Thunnus obesus*) and yellowfin tuna (*Thunnus albacares*) by coupling split-beam echosounder observations and sonic tracking. ICES Journal of Marine Science, 56: 51–60.
- Blackman, S. S. 1986. Multiple Target Tracking with Radar Applications, Artech House, Cambridge, MA.
- Cayré, P., and Laloë, F. 1986. Review of the Gonad Index (GI) and an introduction to the concept of its 'critical value': application to the skipjack tuna *Katsuwonus pelamis* in the Atlantic Ocean. Marine Biology, 90: 345–351.

- Cayré, P., and Chabanne, J. 1986. Marquage acoustique et comportement de thons tropicaux (albacore: *Thunnus albacares*, et listao: *Katsuwonus pelamis*) au voisinage d'un dispositif concentrateur de poissons. *Journal of Tropic Oceanology*, 21: 167–183.
- Clay, A., and Castonguay, M. 1996. In situ target strengths of Atlantic cod (*Gadus morhua*) and Atlantic mackerel (*Scomber scombrus*) in the Northwest. *Canadian Journal of Fisheries and Aquatic Sciences*, 53: 87–98.
- Conti, S. G., Demer, D. A., Soule, M. A., and Conti, J. H. E. 2005. An improved multiple-frequency method for measuring in-situ target strengths. *ICES Journal of Marine Science*, 62: 1636–1646.
- Coull, K. A., Jermyn, A. S., Newton, A. W., Henderson, G. I., and Hall, W. B. 1989. Length/Weight relationships for 88 species encountered in the north-east Atlantic. *Scottish Fisheries Research Report*, 43: 81.
- Cumming, G., Fidler, F., and Vaux, D. L. 2007. Error bars in experimental biology. *The Journal of Cell Biology*, 177: 7–11.
- Demer, D. a., Berger, L., Bernasconi, M., Bethke, E., Boswell, K. M., Chu, D., and Domokos, R., *et al.* 2015. Calibration of acoustic instruments. *ICES Cooperative Research Report*, 326: 133.
- Demer, D. A., Soule, M. A., and Hewitt, R. P. 1999. A multiple-frequency method for potentially improving the accuracy and precision of in situ target strength measurements. *The Journal of the Acoustical Society of America*, 105: 2359–2376.
- Doray, M., Josse, E., Gervain, P., Reynal, L., and Chantrel, J. 2006. Acoustic characterisation of pelagic fish aggregations around moored fish aggregating devices in Martinique (Lesser Antilles). *Fisheries Research*, 82: 162–175.
- Fernandes, A., Masse, J., Iglesias, M., Diner, N., and Ona, E. 2006. The SIMFAMI project: species identification methods from acoustic multi-frequency information. *European Union, Aberdeen, UK*. 486 pp.
- Fonteneau, A., Chassot, E., and Bodin, N. 2013. Global spatio-temporal patterns in tropical tuna purse seine fisheries on drifting fish aggregating devices (DFADs): taking a historical perspective to inform current challenges. *Aquatic Living Resources*, 26: 37–48.
- Foote, K. 1987. Calibration of Acoustic Instruments for Fish Density Estimation: A Practical Guide. *International Council for the Exploration of the Sea, Copenhagen*. 81 pp.
- Forget, F. G., Capello, M., Filmlalter, J. D., Govinden, R., Soria, M., Cowley, P. D., and Dagorn, L. 2015. Behaviour and vulnerability of target and non-target species at drifting fish aggregating devices (FADs) in the tropical tuna purse seine fishery determined by acoustic telemetry. *Canadian Journal of Fisheries and Aquatic Sciences*, 72: 1398–1405.
- Forland, T. N., Hobaek, H., and Korneliussen, R. J. 2014a. Scattering properties of Atlantic mackerel over a wide frequency range. *ICES Journal of Marine Science*, 71: 1904–1912.
- Forland, T. N., Hobaek, H., Ona, E., and Korneliussen, R. J. 2014b. Broad bandwidth acoustic backscattering from sandeel—measurements and finite element simulations. *ICES Journal of Marine Science*, 71: 1894–1903.
- Gauthier, S., and Rose, G. 2001. Diagnostic tools for unbiased in situ target strength estimation. *Canadian Journal of Fisheries and Aquatic Sciences*, 58: 2149–2155.
- Gorska, N., Korneliussen, R. J., and Ona, E. 2007. Acoustic backscatter by schools of adult Atlantic mackerel strength of backbone. *ICES Journal of Marine Science*, 64: 1145–1151.
- Gorska, N., Ona, E., and Korneliussen, R. 2005. Acoustic backscattering by Atlantic mackerel as being representative of fish that lack a swimbladder. Backscattering by individual fish. *ICES Journal of Marine Science*, 62: 984–995.
- Govinden, R., Dagorn, L., Soria, M., and Filmlalter, J. 2010. Behaviour of Tuna associated with drifting fish aggregating devices (FADs) in the Mozambique Channel. *In IOTC 2010 (Seichelles) —WPTT 25*, 22 pp.
- Horne, J. K., Sawada, K., Abe, K., Kreisberg, R. B., Barbee, D. H., and Sadayasu, K. 2009. Swimbladders under pressure: anatomical and acoustic responses by walleye pollock. *ICES Journal of Marine Science*, 66: 1162–1168.
- ICES. 2006. Report of the Working Group on Acoustic and Egg Surveys for Sardine and Anchovy in ICES Areas VIII and IX (WGACEGG). *ICES CM 2010/LRC: 01*. 126 pp.
- ISSF. 2017. ISSF Tuna Stock Status Update, 2017: Status of the world fisheries for tuna. *ISSF Technical Report 2017-02*. *International Seafood Sustainability Foundation, Washington, DC, USA*.
- Jech, J. M., Horne, J. K., Chu, D., Demer, D. A., Francis, D. T. I., Gorska, N., and Jones, B. 2015. Comparisons among ten models of acoustic backscattering used in aquatic ecosystem research. *Journal of the Acoustical Society of America*, 138: 3742–3764.
- Johnson, S. G. (n.d.). The NLOpt nonlinear-optimization package.
- Josse, E., and Bertrand, A. 2000. In situ acoustic target strength measurements of tuna associated with a fish aggregating device. *ICES Journal of Marine Science*, 57: 911–918.
- Korneliussen, R. 2010. The acoustic identification of Atlantic mackerel. *ICES Journal of Marine Science*, 67: 1749–1758.
- Korneliussen, R. J., Heggelund, Y., Macaulay, G. J., Patel, D., Johnsen, E., and Eliassen, I. K. 2016. Acoustic identification of marine species using a feature library. *Methods in Oceanography*, 17: 187–205.
- Lawson, G. L., Barange, M., Freon, P., and Fre, P. 2001. Species identification of pelagic fish schools on the South African continental shelf using acoustic descriptors and ancillary information. *ICES Journal of Marine Science*, 58: 275–287.
- Lopez, J., Moreno, G., Boyra, G., and Dagorn, L. 2016. A model based on data from echosounder buoys to estimate biomass of fish species associated with fish aggregating devices. *Fishery Bulletin*, 114: 166–178.
- Lopez, J., Moreno, G., Sancristobal, I., and Murua, J. 2014. Evolution and current state of the technology of echo-sounder buoys used by Spanish tropical tuna purse seiners in the Atlantic, Indian and Pacific Oceans. *Fisheries Research*, 155: 127–137. Elsevier B.V.
- MacLennan, D., and Menz, A. 1996. Interpretation of in situ target-strength data. *ICES Journal of Marine Science*, 53: 233.
- MacLennan, D. N., Fernandes, P. G., and Dalen, J. 2002. A consistent approach to definitions and symbols in fisheries acoustics. *ICES Journal of Marine Science*, 59: 365–369.
- Marsac, F., and Cayré, P. 1998. Telemetry applied to behaviour analysis of yellowfin tuna (*Thunnus albacares*, Bonnaterre, 1788) movements in a network of fish aggregating devices. *Hydrobiologia*, 371/372: 155–171.
- Misund, O. 1993. Dynamics of moving masses: variability in packing density, shape, and size among herring, sprat, and saithe schools. *ICES Journal of Marine Science*, 50: 145–160.
- Misund, O., and Beltestad, A. 1996. Target-strength estimates of schooling herring and mackerel using the comparison method. *ICES Journal of Marine Science*, 53: 281–284.
- Moreno, G., Dagorn, L., Capello, M., Lopez, J., Filmlalter, J., Forget, F., Sancristobal, I., *et al.* 2016. Fish aggregating devices (FADs) as scientific platforms. *Fisheries Research*, 178: 122–129.
- Moreno, G., Josse, E., Brehmer, P., Nøttestad, L., and Us, C. D. B. 2008. Echotracer classification and spatial distribution of pelagic fish aggregations around drifting fish aggregating devices (DFAD). *Aquatic Living Resources*, 356: 343–356.
- Mosteiro, A., Fernandes, P. G., Armstrong, E., and Greenstreet, S. 2004. A dual frequency algorithm for the identification of sandeel school echotraces. *ICES CM2004/R:12*. 13 pp.
- Muir, J., Itano, D., Hutchinson, M., Leroy, B., and Holland, K. 2012. Behavior of target and non-target species on drifting FADs and

- when encircled by purse seine gear. *In* Western and Central Pacific Fisheries Commission—Scientific Committee, Busan, Republic of Korea, 8 pp.
- Oshima, T. 2008. Target strength of Bigeye, Yellowfin and Skipjack measured by split beam echo sounder in a cage. IOTC, WPTT-22, 4 pp.
- Powell, M. 1994. A direct search optimization method that models the objective and constraint functions by linear interpolation. *Advances in Optimization and Numerical Analysis*, 275: 51–67.
- R Core Team. 2014. R: A language and environment for statistical computing. R Foundation for Statistical Computing, Vienna, Austria.
- Sawada, K., Furusawa, M., and Williamson, N. J. 1993. Conditions for the precise measurement of fish target strength *in situ*. *Fisheries Science (Tokyo)*, 20: 15–21.
- Scoulding, B., Gastauer, S., Maclellan, D. N., Fässler, S. M. M., Copland, P. J., and Fernandes, P. G. 2016. Effects of target strength variability on estimates of abundance: The case of Atlantic mackerel (*Scomber scombrus*). *Journal of the Acoustical Society of America*, 140: 3243.
- Seber, G. 1982. Estimation of Animal Abundance and Related Parameters. Macmillan, New York.
- Sigfusson, H., Decker, E. A., and McClements, D. J. 2001a. Ultrasonic characterization of Atlantic mackerel (*Scomber scombrus*). *Food Research International*, 34: 15–23.
- Sigfusson, H., Decker, E. A., Morrissey, M., and McClements, D. J. 2001b. Ultrasonic characterization of north Pacific Albacore (*Thunnus alalunga*). *Journal of Aquatic Food Product Technology*, 10: 5–20.
- Simmonds, J. E., and Maclellan, D. N. 2005. *Fisheries Acoustics Theory and Practice*, 2nd edn. Chapman & Hall, New York. 472 pp.
- SIMRAD. 1996. Simrad EK500 Scientific Echosounder Instruction Manual. Simrad Subsea A/S, Horten, Norway.
- Soule, M., Barange, M., Solli, H., and Hampton, I. 1997. Performance of a new phase algorithm for discriminating between single and overlapping echoes in a split-beam echosounder. *ICES Journal of Marine Science*, 54: 934–938.
- Sueur, J., Aubin, T., and Simonis, C. 2013. Seewave: a free modular tool for sound analysis and synthesis. *Bioacoustics*, 18: 213–226.

Handling editor: Purnima Ratilal